Journal of the European Ceramic Society 22 (2002) 1403–1409

www.elsevier.com/locate/jeurceramsoc

Extraction of binders from green ceramic bodies by supercritical fluid: influence of the porosity

Thierry Chartier*, Fleur Bordet, Eric Delhomme, Jean François Baumard

Laboratoire des Matériaux Céramiques et Traitements de Surface, UMR-CNRS 6638, SPCTS-ENSCI, 87065 Limoges cedex, France

Received 8 June 2001; received in revised form 27 September 2001; accepted 7 October 2001

Abstract

Organic additives can be extracted from extruded or injection-moulded ceramic parts by using supercritical fluids leading to defect free green parts in a short time. A model previously defined, that predicts kinetics of extraction of solid binder molecules by solubilization and diffusion of solubilized species has been modified with a corrective term taking into account the capillary migration of a liquid organic phase according to the microstructure (pore size distribution, tortuosity) of the green sample and to the characteristics of the liquid phase (viscosity, surface tension). An analytical expression of this corrective term is proposed, for a paraffin binder and for three alkanes which are representative of its molecular distribution. The corrective term is related to the length scale over which the liquid binder flow occurs and to its linear velocity. The modified model allows the prediction of the kinetics of extraction of a given paraffin binder, by using the effective diffusion coefficient of the binder, determined with large pore size green samples and a capillary factor, calculated from binder and microstructure characteristics of the green part.

Keywords: Debonding; Diffusion; Green bodies; Modelling; Porosity; Supercritical fluids

1. Introduction

Most high technology ceramic processing like dry-pressing, tape-casting, extrusion or injection-moulding requires the use of organic compounds (dispersants, binders, plasticizers) to confer such properties as cohesion, flexibility and workability in the green state. Amounts as large as 50 vol.% of organic additives can be added to the ceramic powder during the forming step. Thermal decomposition is currently used to remove the organic phase but is very time-consuming[1–4] and may lead to the formation of defects which subsequently affect properties of the sintered samples.[5] Extraction of binders by supercritical fluids, based on the unique solvent power and transport properties of such fluids at temperatures and pressures beyond their critical point,[6] has proven to be an interesting alternative way to reduce the debinding time and also to produce defect-free green bodies.[7,8] Supercritical CO_2 is the most extensively used fluid (in the food or perfume industry) and has shown promising possibilities for the extraction of "light" organic compounds in ceramic forming processes. The main advantages of carbon dioxide lie in a low cost as well as in the absence of toxicity and flammability.

According to previous studies,[9,10] two mechanisms take place in the extraction of organic additives in the solid state, namely solubilization of binder molecules and diffusion of solubilized species. A third mechanism involving capillary migration takes place when the organic phase is in a liquid state.

A model, based on the classical diffusion equations, has been developed to predict the kinetic of extraction of a soluble solid binder in supercritical CO_2.[10] In the case of a porous ceramic cylinder of radius R(m) with an infinite length ($L \gg R$), the mass fraction of polymer which subsists in the green body, after time t of extraction, can be expressed by:

$$\frac{C_t}{C_0} = \frac{4}{R^2} \sum_{n=1}^{\infty} \frac{1}{\beta_n^2} \exp(-D\beta_n^2 t) \quad (1)$$

where C_0 is the initial binder concentration, C_t the binder remaining concentration at time t of extraction, D the diffusivity ($m^2\ s^{-1}$) of the dissolved binder molecules

* Corresponding author. Tel.: +33-5-5545-2222; fax: +33-5-5579-0998.

E-mail address: t.chartier@ensci.fr (T. Chartier).

0955-2219/02/$ - see front matter
PII: S0955-2219(01)00474-5

supposed constant during the extraction and β_n the root of $J_0(\beta_n R)=0$, where J_0 is the first order kind Bessel function of order 0. This model is only based on the diffusion of solubilized species throughout the ceramic body, that is the limiting mechanism in the case of a solid organic phase. For a solid binder, molecules are solubilized in the body and diffuse in the pores filled with the binder phase and/or with the supercritical fluid phase depending on the advancement of the extraction. The diffusion of solubilized molecules in the supercritical fluid phase may be several orders of magnitude higher than the diffusion of solubilized molecules in the binder phase.

This model is in good agreement with experimental results for a solid binder but is no more valid in the case of a binder in liquid state. It does not take into account the capillary migration that constitutes the major contribution of the extraction for a liquid organic phase and that is function of binder characteristics (viscosity, surface tension, wetting properties) and of the sample microstructure (pore size distribution, tortuosity). When the binder is liquid, it redistributes from the large pores in the body to the small pores at the surface as long as the binder phase is not localised in isolated pockets. During this step, the solubilization at the surface still controls the extraction process. When the binder phase becomes disconnected (pendular regime), diffusion of the various solubilized molecules in supercritical CO_2 controls the process.

The aim of this study mainly concerns the influence of the pore size of green alumina samples on the extraction rate, by supercritical carbon dioxide, of a liquid paraffin binder and of three alkanes representative of the composition of this paraffin (C_{22}, C_{28} and C_{36}). Paraffin waxes are commonly used as binders in extrusion or injection-moulding formulations. The final objective is to relate the extraction of the alkanes to the extraction of the paraffin and then to be able to predict the paraffin binder behaviour during the supercritical treatment, knowing its composition.

2. Experimental procedure

2.1. Materials

Different alumina powders (99.7% purity) supplied by Aluminium Péchiney (Gardanne, France) were used. The mean particle size and the specific surface area of these powders (Table 1) were chosen in order to obtain different mean pore diameters as well as a narrow pore size distribution of the green samples.

One paraffin binder that melts at 42 °C (paraffin 42, with a molecular distribution centred on alkane C_{22}, Aldrich, France) and three alkanes (C_{22}, C_{28} and C_{36}), representative of the large paraffin 42 molecular repartition (92% of the constitutive alkanes are comprised between C_{18} and C_{30}), were used.

Table 1
Mean particle sizes and specific surface areas of the alumina powders used

Alumina grade	AC34	P122B	P152	P152SB	P172SB
Specific surface area ($m^2\ g^{-1}$)	–	1.1	1.6	3.5	10.0
Mean particle size (μm)	30	5.0	1.7	1.0	0.5

2.2. Forming of ceramic bodies with different pore sizes

To obtain controlled porosity with reliable values (volume and pore size), porous pre-sintered alumina samples were first prepared then filled with the paraffin or with one of the alkanes by infiltration under vacuum.

Green alumina disks (50 mm height, 25 mm diameter) were obtained by dry-pressing (150 MPa) the different alumina grades, previously spray dried (Laboratory spray-dryer, Büchi 190, Germany). The aqueous suspension for spray drying contained 59 wt.% alumina powder, 0.45 wt.% dispersant (PMAA-NH_4^+, Darvan C, Vanderbilt, UK) and 1.75 wt.% binder (PEG 20M, Union Carbide, USA). Dispersant and binder concentrations are expressed on a dry weight alumina basis. The mean size of spray-dried granules was about 30 μm.

In order to confer the pressed samples enough cohesion for paraffin or alkane infiltration without modifying their pore size, they were pre-sintered, after debinding (0.5 °C min^{-1} up to 400 °C—30 min dwell-time), at 5 °C min^{-1} up to the temperature at which particles just begin to bond to each other. This stage corresponds to the neck formation between particles and to the beginning of shrinkage. Pre-sintering temperatures were determined for each powder by dilatometric measurements (Table 2). In the specific case of very low pore size (lower than 0.1 μm), some P172SB alumina samples were pre-sintered at 1450 °C during a 6 min dwell-time.

Samples with a large pore diameter (about 10 μm) were prepared to be considered as reference ceramic bodies with no significant influence of the microstructure on the extraction rate. To obtain large pores, dense alumina agglomerates (calcined AC34 grade, Table 1) with the addition of a glassy phase were used. Pressed disks were pre-sintered up to 700 °C with a 4 h dwell-time to ensure the cohesion of the porous compact.

Before impregnation, the mean pore diameter, the total porosity and the pore size distribution of each sample were measured by mercury porosimetry (Autopore II, Micromeritics, France) (Table 2, Fig. 1).

In order to determine the influence of supercritical CO_2 on the melting temperature of paraffin 42 and of the three alkanes C_{22}, C_{28} and C_{36} (plasticizing effect), cylinders of pure paraffin wax or alkanes were prepared by pouring the liquid binder in a cylinder.

Table 2
Treatment temperature, mean pore diameter and porosity of the pre-sintered ceramic porous bodies prepared for paraffin and alkane infiltrations

Alumina grade	P172SB	P172SB	P152SB	P152	P122B	Dense AC34 Agglomerates/glass
Treatment temperatures (°C)	1450	900	950	950	1050	700
Porosity (vol.%)	14.9	39.6	39.0	46.4	43.3	67.0
Mean pore diameter (μm)	0.09	0.12	0.30	0.70	0.80	8.97

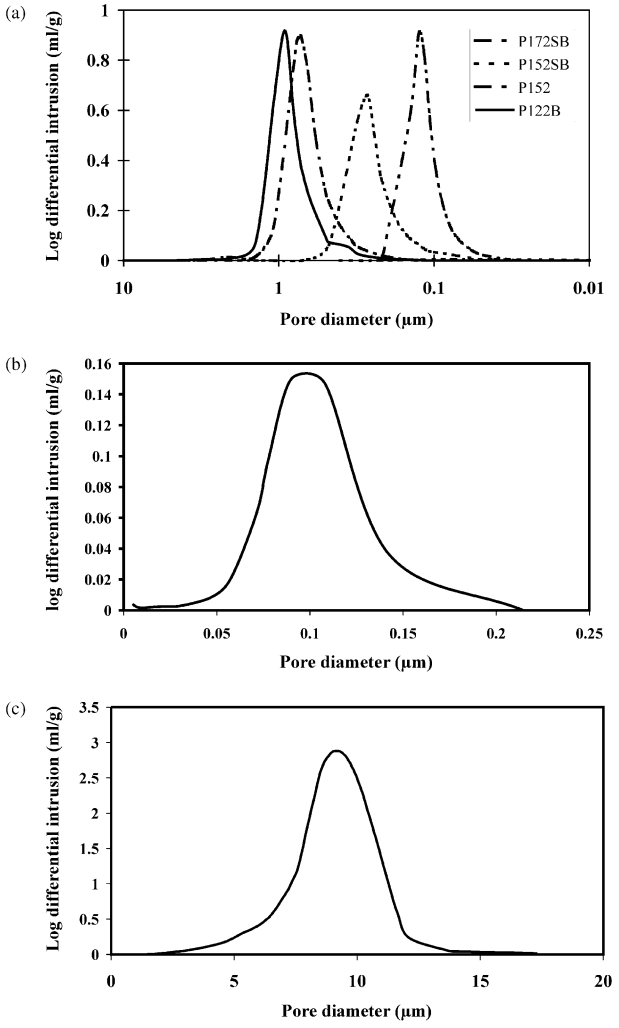

Fig. 1. Pore size distribution of the ceramic porous bodies prepared for paraffin 42 and alkanes infiltrations, (a) P172SB, P152SB, P152 and P122B alumina grades pre-sintered for 10 min at 900, 950, 950 and 1050 °C, respectively, (b) P172SB alumina pre-sintered at 1450 °C for 6 min, (c) dense AC34 agglomerates/glass pre-sintered at 700 °C for 4 h.

2.3. Infiltration

The paraffin and alkanes infiltration process was performed at 110 °C under vacuum in a glass vessel fitted with a valve allowing the paraffin or the alkane to flow on the porous bodies. Vacuum was maintained as long as small air bubbles escaped from the ceramic bodies to ensure a good penetration. Infiltrated samples were finally removed and carefully cleaned to eliminate the excess of paraffin remaining on the surfaces.

2.4. Debinding experiments

Extraction of the paraffin wax and of the alkanes was performed by using supercritical CO_2. The equipment used for this study has been described elsewhere.[1] The extraction can be operated up to 30 MPa, at temperatures ranging from 30 to 120 °C. The cell temperature is regulated within ±1 °C and the pressure within ±0.2 MPa. The flow rate of CO_2 used during the experiments was set to 2.5 l h^{-1}, that avoids any problem of confinement.

Infiltrated samples were weighed and placed in the extraction vessel. They were treated under 28 MPa, at 40 and 70 °C, for 30 min. All these experiments were repeated two times, using new infiltrated alumina samples at each time.

The experimental average fraction of organic removed ($\alpha = 1 - \frac{C_t}{C_0}$), after a treatment time t, was calculated from the weight change of the sample.

3. Results and discussion

3.1. Plasticizing effect of the supercritical carbon dioxide

A first point was to verify the physical state (liquid or solid) of the paraffin 42 and of the three alkanes under experimental conditions. The melting point of an organic binder in a supercritical environment may differ from its melting point in air, due to the plasticizing effect of supercritical fluid (CO_2 in our case).[11] The physical state of cylinders of the paraffin 42 and of the pure alkanes were determined, under 28 MPa at 40 and 70 °C, by a visual observation in a cell through a sapphire window. At 40 °C, cylinders of paraffin and of C_{22} swelled and cylinders of C_{28} and C_{36} were unchanged. Alkane C_{22} is considered liquid and the alkanes C_{28} and C_{36} solid at 40 °C. At 70 °C, the paraffin 42 and the three alkanes were swollen and are then considered liquid.

3.2. Influence of the porosity

Experimental mass fraction of binders removed under 28 MPa at 40 and 70 °C, for different porosities, are

given in Table 3. These values are mean values of two samples tested for each debinding condition. Experimental errors associated with the extraction device (pressure and temperature regulations, CO_2 flow rate) and with the weight loss measurement lead to an absolute variation on the extraction rate that varies from ± 0.01 for the smallest pore volume samples (14.9 vol.% for the 0.09 μm pore size) to ± 0.1 for the highest pore volume ones (67 vol.% for the 9 μm pore size).

Whatever the physical state of the organic phase (solid or liquid), under constant extraction conditions, the organic mass fraction removed increases as the mean pore diameter increases up to 0.8 μm pore size and remains almost constant for larger pore size (9 μm). As the solubility of organic molecules in supercritical CO_2 is independent on the microstructure, the increase of the mass fraction removed with the pore size can be likely related to a better diffusion of dissolved species and/or to a higher capillary migration when the organic phase is liquid. In order to develop a model able to predict the kinetic of extraction of a liquid binder by supercritical CO_2, then taking into account the capillary contribution, we will now consider the organic in the liquid state.

3.3. Extraction of liquid binder

When the organic is in a liquid state (the paraffin at $T = 40$ and 70 °C, the light alkane C_{22} at 40 and 70 °C and the alkanes C_{28} and C_{36} at $T = 70$ °C), molecules are removed from the body not only by solubilization in the supercritical fluid and diffusion of solubilized species in the liquid organic phase or in the supercritical fluid present in the porosity of the sample, but also by capillary migration. Thus, it is important to quantify the capillary phenomenon that occurs in the porous green ceramic body.

When the binder is in a liquid state, it is submitted to a capillary force that drains the liquid, from large pores to small pores, and to a viscous one that tends to hinder the liquid movement. When the capillary force is greater than the viscous force, flow of molten binder occurs. As a result, the small pores near the surface of the body are continuously supplied with molten binder from the larger pores located within the body. Thus, diffusion paths of binder molecules, flowing from these large pores and solubilized either at the surface of the sample or in the small pores, near the surface, are considerably shorter and the extraction rate increases when liquid flow takes place.

The capillary movement of the molten binder is due to the capillary pressure difference ΔPc that exists between pores of different diameters:[12]

$$\Delta Pc = 2\gamma\cos\theta\left(\frac{1}{R_1} - \frac{1}{R_2}\right) \quad (2)$$

where γ is the surface tension of the liquid (equal to 3.10^{-3} N.m^{-1} for the paraffin and alkanes used at 70 °C, as a first approximation), θ is the contact angle (equal to 0 as the paraffin and alkanes do poorly wet alumina powders), R_1 is the radius of the small pore (m) and R_2 is the radius of the large pore (m). R_1 and R_2 were respectively taken equal to the d_{10} and the d_{90} values in the pore size distribution (Fig. 1). d_{10} and d_{90} are the particle sizes corresponding to 10 vol.% and 90 vol.% of particles with a size lower than d_{10} and d_{90}, respectively.

Table 3
Experimental mass fractions ($\alpha = 1 - \frac{C_t}{C_0}$) of paraffin wax and of alkanes removed from the alumina samples for 30 min under 28 MPa at 40 and 70 °C (l: liquid state; s: solid state)

Organic	Porosity (μm)	Mass fraction of binder removed ($\alpha = 1 - \frac{C_t}{C_0}$) after $t = 30$ min	
		40 °C	70 °C
C_{22}	0.09	0.50±0.02 (l)	0.58±0.02 (l)
	0.3	0.89±0.025 (l)	0.85±0.025 (l)
	0.8	0.90±0.05 (l)	0.90±0.05 (l)
	9	0.90±0.1 (l)	0.91±0.1 (l)
C_{28}	0.09	0.12±0.015 (s)	0.54±0.015 (l)
	0.3	0.27±0.025 (s)	0.73±0.025 (l)
	0.8	0.35±0.05 (s)	0.85±0.05 (l)
	9	0.40±0.1 (s)	0.90±0.1 (l)
C_{36}	0.09	0.04±0.01 (s)	0.10±0.01 (l)
	0.3	0±0.025 (s)	0.12±0.025 (l)
	0.8	0±0.05 (s)	0.13±0.05 (l)
	9	0±0.1 (s)	0.20±0.1 (l)
Wax 42	0.09	0.20±0.02 (l)	0.46±0.02 (l)
	0.30	0.67±0.025 (l)	0.73±0.025 (l)
	0.80	0.78±0.05 (l)	0.87±0.05 (l)
	9	n.d.	0.90±0.1 (l)

Capillary pressure differences ΔPc, calculated for each sample Eq. (2), are given in Table 4.

The pressure drop ΔPv during the liquid displacement due to viscous losses is given by the following equation:[12]

$$\Delta Pv = \frac{36K\eta}{d_{50}^2}\frac{(1-\varepsilon)^2}{\varepsilon^3}hu_c \quad (3)$$

where K (generally equal to 5)[13] is a constant named "tortuosity", d_{50} is the mean particle diameter (m), ε the relative porosity, η the viscosity of the binder, h the distance over which flow occurs (m) and u_c ($u_{capillary}$) the linear velocity of the liquid binder (m s^{-1}).

Flow occurs if the pressure difference between two pores is greater than the pressure drop due to the viscosity of the fluid, thus if ΔPc is greater than ΔPv. To judge the length scale over which flow occurs and the linear velocity of the molten fluid, Eqs. (2) and (3) can be equated to give:

$$hu_c = \frac{2\gamma\cos\theta}{36K\eta}\left(\frac{1}{d_{10}}-\frac{1}{d_{90}}\right)\frac{\varepsilon^3}{(1-\varepsilon)^2}d_{50}^2 \quad (4)$$

Values of viscosities considered under atmospheric pressure and at 70 °C are equal to 5×10^{-3} Pas for the paraffin and to 10^{-3}, 4×10^{-3} and 6.3×10^{-3} Pas for the alkanes C_{22}, C_{28} and C_{36}, respectively. Under 28 MPa, in supercritical CO_2, the values of viscosity are unknown as the supercritical CO_2 may modify this value but we will suppose the viscosity values remain constant for a qualitative approach keeping in mind that these values are over-estimated because of the plasticizing effect of the supercritical carbon dioxide. Values of hu_C verifying Eq. (4) were calculated for each alkane and for the paraffin in the porosity range tested (i.e. 0.09–9 μm) (Table 5). The hu_c values, then the extraction rates, decrease when the viscosity of the binder increases. The hu_c values for the paraffin are closest to the values of alkane C_{28} than to the values of alkane C_{22} whereas the wax composition is centred on the C_{22} alkane. This can be attributed to the viscosity of paraffin 42 (5×10^{-3} Pa.s) similar to that of alkane C_{28} (4×10^{-3} Pa s) and higher to the viscosity of alkane C_{22} (10^{-3} Pa s).

Table 4
Capillary pressure difference, at 70 °C, calculated [Eq. (2)] between the largest (d_{90}) and the smallest (d_{10}) pores of each pore size distribution (d_{10} and d_{90} are the particle size corresponding to the 10 and 90 vol.% of particles with a size lower than d_{10} and d_{90}, respectively)

Mean pore diameter (μm)	ΔPc (Pa)	d_{10} (μm)	d_{90} (μm)
0.09	7.5×10^4	0.06	0.18
0.12	4.2×10^4	0.07	0.14
0.30	3.0×10^4	0.14	0.48
0.70	1.8×10^4	0.34	1.08
0.80	8.1×10^3	0.49	1.43
9.00	1.2×10^3	5	12

Table 5
hu_c Values calculated in the 0.09–9 μm porosity range (according to the pore size distribution) at 70 °C [Eq. (4)]

	Mean pore diameter (μm)	hu_c (m^2 s^{-1})
C_{22}	0.09	1.5×10^{-11}
	0.30	2.4×10^{-9}
	0.80	7.2×10^{-9}
	9	7.5×10^{-6}
C_{28}	0.09	3.8×10^{-12}
	0.30	6×10^{-10}
	0.80	1.8×10^{-9}
	9	1.9×10^{-6}
C_{36}	0.09	2.5×10^{-12}
	0.30	1.6×10^{-10}
	0.80	4×10^{-10}
	9	1.2×10^{-6}
Wax 42	0.09	3.1×10^{-12}
	0.30	4.8×10^{-10}
	0.80	1.5×10^{-9}
	9	1.5×10^{-6}

For each sample and each organic at 70 °C (temperature for which alkanes and wax are liquid), hu_c values are increasing with the pore size. The hu_c parameter represents the capillary migration of the binder and depends on geometrical factors of the ceramic body and on the characteristics of the organic phase (viscosity, surface tension, wetting properties) and is, in a first approximation, independent on the diffusion of solubilized species. Then hu_C values allow estimating the influence of the structure of the green body on the liquid binder migration.

3.4. Extraction model extended to a liquid binder

In order to take into account the influence of the microstructure of the green part on the extraction rate of a liquid binder, a corrective term A, which represents the braking effect of the microstructure on the capillary movement of liquid binder, can be introduced in Eq. (1):

$$\frac{C_t}{C_0} = \frac{4}{R^2}\sum_{n=1}^{\infty}\frac{1}{\beta_n^2}\exp(-D_e\beta_n^2 t) - A \quad (5)$$

where D_e is an effective diffusion coefficient (m^2 s^{-1}), independent on the microstructure.

If we consider that extraction rates obtained with the largest pore size samples (9 μm) are effective extraction rates without effect of the microstructure, then A can be taken equal to 0 for 9 μm pore size samples.

Experimental values of A were then simply determined by the difference between the mass fractions removed from the 9 μm pore size sample, for which no braking effect is considered, and mass fractions removed

from the considered low pore size samples, for which the microstructure influences the extraction. Table 6 gives values of the experimental term A, for liquid C_{22}, C_{28} and C_{36} alkanes and for liquid wax 42 for which capillary migration prevails at 70 °C. Small pore size greatly influences the extraction rate of liquid binders.

As the term A is representative of the braking effect of the microstructure, it could be likely related to the values of hu_c for each considered organic. Experimental values of A have been related to calculated hu_c values ($m^2\ s^{-1}$) for each porosity lower than 9 μm (i.e. 0.09, 0.3 and 0.8 μm) by the following expressions (data regression):

$$\ln A_{C22=} - 0.49 \ln hu_c - 13.3 \quad (6)$$

$$\ln A_{C28} = -0.27 \ln hu_c - 7.9 \quad (7)$$

$$\ln A_{C36} = -0.06 \ln hu_c - 4 \quad (8)$$

$$\ln A_{wax\ 42=} - 0.32 \ln hu_c - 9.3 \quad (9)$$

The mobility of liquid alkane is decreasing when the viscosity is increasing then, when the number of carbon of the alkane is increasing. The slope of (ln A) versus (ln hu_C) increases (approaches 0) for high carbon number of the alkane. The slope value of wax 42 (−0.32) is closest to the slope value of C_{28} alkane (−0.27) than to the slope value of C_{22} alkane (−0.49) whereas the wax composition is centred on the C_{22} alkane. As for the hu_c values (paragraph 3.3), this can be attributed to the viscosity of wax 42 which is close to that of C_{28} alkane.

In the case of the paraffin 42, expression (5) could be written using the analytical expression of A defined for this binder [expression (9)]. This expression offers the advantage to predict the kinetic of extraction of the paraffin 42 binder from a green sample and then to be able to adjust the experimental conditions. This approach can be extended to other binders and to different green part microstructures. Parameters to be known are the effective diffusion coefficient of the considered paraffin binder, determined by using large pore size samples, and hu_C values calculated from paraffin binder and microstructure characteristics.

Expressions (6)–(9) also suggest that it could be possible to predict the corrective term A of a paraffin binder, knowing its alkanes repartition, for a given green sample (fixed microstructure). This model has to take into account the alkane concentration in the paraffin and corrective term of each alkane of the paraffin distribution, or at least corrective terms of some representative alkanes.

Table 6
Effect of the microstructure on the extraction rate. The corrective terms A [Eq. (5)], for the liquid alkanes C_{22}, C_{28}, C_{36} and paraffin 42 (28 MPa, $T = 70$ °C, $t = 30$ min), were simply determined by the difference between the mass fractions removed from the 9 μm pore size samples, for which there is no braking effect, and mass fractions removed from the considered low pore size samples, for which microstructure influences the extraction

	Porosity (μm)	Mass fraction removed ($\alpha = 1 - \frac{C_t}{C_0}$)	A exp.
C_{22}	0.090.30.89	0.580.850.90.91	0.330.060.010
C_{28}	0.090.30.89	0.540.730.850.9	0.360.170.050
C_{36}	0.090.30.89	0.10.120.130.2	0.10.080.070
Wax 42	0.090.30.89	0.460.730.870.9	0.440.170.030

4. Conclusion

Several parameters are governing the extraction process of binder by supercritical fluids. Some are related to the physical state of the binder, under critical conditions, liquid or solid, that is influenced by the plasticizing effect of the supercritical carbon dioxide. Others are related to the experimental conditions of extraction. At low temperature and under high pressures, solubilization is predominant whereas at high temperatures, diffusion and capillary migration prevail. Among these parameters, the microstructure (porosity) of the green ceramic bodies greatly influences the mass fractions of binder removed, mainly when the binder is in a liquid state due to capillary migration.

Capillary phenomenon has a great influence on extraction, when the binder is in the liquid state. For example, in the case of the alkane C_{28}, at 28 MPa, for a 9 μm pore size, mass fraction of binder removed increases by a factor 2.25 from a solid state to a liquid one for which the capillary phenomenon could occur.

For small pore sizes, microstructure of the sample significantly brakes the extraction rate. For the 0.09 μm pore size, the diminution of the extraction rate varies from 36 to 49% according to the considered organic in comparison to large pore size (9 μm). In order to take into account the capillary migration, and particularly the influence of the porosity, a corrective term has been introduced in the previously defined expression of extraction rate, only based on the diffusion of dissolved species, then theoretically only valid for solid binders. An analytical expression of this corrective term allows to predict the kinetic of extraction of a given paraffin binder from a green sample by knowing its effective diffusion coefficient, determined by using large pore size samples, and a capillary kinetic factor, calculated from the considered binder properties and from the green sample microstructure characteristics. Expressions of this corrective term are given for the studied paraffin binder (melting point of 42 °C) and for three alkanes representative of this paraffin molecular distribution. Then, it becomes likely possible to approach the corrective term of a paraffin binder using the expressions of the corrective

terms of the alkanes representative of the considered paraffin molecular distribution.

Acknowledgements

The authors are grateful to ADEME and Region Limousin for their financial support.

References

1. Zangh, J. G., Edirisinghe, M. J. and Evans, J. R. G., A catalogue of ceramic injection moulding defects and their causes. *Ind. Ceram*., 72–82.
2. Lange, F. F., Davis, B. I. and Wright, E. J., Processing related fracture origins: IV, elimination of voids produced by organic inclusions. *J. Am. Ceram. Soc*., 1989, **69**, 66–69.
3. Bennison, S. J. and Harmer, M. P., Swelling of hot-pressed alumina. *J. Am. Ceram. Soc*., 1989, **68**, 591–596.
4. Dong, C. and Bowen, H. K., Hot stage bubble formation during binder burnout. *J. Am. Ceram. Soc*., 1989, **72**, 1082–1087.
5. Pinwill, I. E., Edirisinghe, M. J. and Bevis, M. J., Development of temperature heating rate diagrams for the pyrolytic removal of binder used for powder injection moulding. *J. Mater. Sci*., 1992, **27**, 4381–4388.
6. Rosset, R. and Perrut, M., La chromatographie avec éluant supercritique. In *Proceedings of the International Symposium on Supercritical Fluids*. INPL Press, Vandoeuvre, France, 1987, pp. 305–322.
7. Miyashita, T., Ueno, U. and Kubodera, S., *Method for Removing the Dispersion Medium from a Moulded Pulverulent Material*. US Patent No. 4737332, 1988.
8. Nakashima, N., Nishikawa, E. and Wakao, N., Binder removal from a ceramic green body in the environment of supercritical carbon dioxide with/without entrainers. In *Proceedings of the 2nd International Symposium on Supercritical Fluids*, ed. M. McHugh. Butterworth, Boston, MA, 1991, pp. 357–359.
9. Chartier, T., Ferrato, M. and Baumard, J. F., Supercritical debinding of injection moulded ceramics. *J. Am. Ceram. Soc*., 1995, **78**, 1787–1792.
10. Chartier, T, Delhomme, E. and Baumard, J. F., Mechanisms of binder removal involved in supercritical debinding of injection-moulded ceramics. *J. Phys. III*, 1997, **7**, 291–308.
11. Schnitzler, J. V. and Eggers, R., Mass transfer phenomena in polymers during treatment in a supercritical CO_2 atmosphere. Proceedings of the 5th meeting on Supercritical Fluids. INPL Press: Vandoeuvre, France, 1998, pp. 93–98.
12. Cima, M. J., Lewis, J. A. and Devoe, A. D., Binder distribution in ceramic greenware during thermolysis. *J. Am. Ceram. Soc*., 1989, **72**, 1192–1199.
13. Satterfield, C. N., *Mass Transport in Heterogeneous Catalysis*. MIT Press, Cambridge, 1970.